Acta Crystallographica Section D
Biological Crystallography
ISSN 0907-4449

Purification and crystallization of the yeast translation elongation factor eEF3

Christian Folsted Andersen,[a] Monika Anand,[b] Thomas Boesen,[a] Lan Bich Van,[a] Terri Goss Kinzy[b,c] and Gregers Rom Andersen[a]*

[a]Department of Molecular Biology, University of Aarhus, Gustav Wieds Vej 10C, DK-8000 Aarhus, Denmark, [b]Department of Molecular Genetics, Microbiology and Immunology, Robert Wood Johnson Medical School, Piscataway, New Jersey, USA, and [c]The Cancer Institute of New Jersey, USA

Correspondence e-mail: grand@imsb.au.dk

Received 4 March 2004
Accepted 4 May 2004

A *Saccharomyces cerevisiae* strain expressing full-length histidine-tagged translation elongation factor 3 (eEF3) as the only form of the protein facilitated purification of the factor for both structural and functional studies. Additionally, an identical full-length form has been successfully expressed in *Escherichia coli* and a C-terminally truncated form of histidine-tagged eEF3 has been successfully expressed in *E. coli* and *S. cerevisiae*. Both forms have been crystallized and crystals of the truncated protein expressed in yeast diffract synchrotron radiation to a maximum resolution of 2.3 Å. A density-modified map derived from low-resolution SIRAS phases allows model building.

1. Introduction

The last step of gene expression, the production of the polypeptide, can be separated into distinct phases of initiation, elongation and termination (reviewed in Merrick & Hershey, 1996). Each of these steps is performed on the ribosome but facilitated by the action of a series of soluble protein-synthesis factors. These factors are critically important in the regulation of protein synthesis. Translation begins when an initiator Met-tRNA$_i$ is deposited at a specific AUG codon in the 80S ribosome. Each subsequent amino acid is delivered to the ribosome as an aminoacyl-tRNA (aa-tRNA) and peptide-bond formation is accomplished by the activity of the ribosome. The growing peptidyl-tRNA is moved along the mRNA by the action of a translocase (eEF2 in eukaryotes). When a stop codon is encountered, termination of the polypeptide chain occurs.

The protein-synthetic apparatus is in many ways highly conserved in eukaryotic species, although there are unique differences between fungi and metazoans. Many of these differences are in the composition but not necessarily the function of translation elongation factors (eEFs). In fungi, the most unique difference is the presence of a third essential elongation factor, eEF3. eEF3 is an ATP-binding protein that promotes the release of deacylated tRNA from the E-site, thereby increasing the affinity of aa-tRNA for the A-site (Triana-Alonso *et al.*, 1995). The protein also physically and genetically interacts with eEF1A (Anand *et al.*, 2003).

As an essential component of fungal protein synthesis *in vitro* and *in vivo*, eEF3 and its interactions with the translational apparatus are potential targets for drug discovery. Fungal-specific proteins such as eEF3 are possible antifungal drug targets (Sturtevant, 2002). Thus, functional and structural studies have the potential to direct the development of new antifungal compounds.

Structural studies of prokaryotic elongation factors have generated key knowledge on the mechanism of protein synthesis. Recent studies have begun to bring our structural understanding of eukaryotic translation elongation to the level previously known only for the prokaryotic factors, including the NMR structure of the C-terminus of eEF1Bα (Pérez *et al.*, 1999), the high-resolution X-ray crystal structures of eEF1A in complex with the C-terminus of eEF1Bα (Andersen *et al.*, 2000), eEF2 (Jørgensen *et al.*, 2003) and the N-terminus of eEF1Bγ (Jeppesen *et al.*, 2003). Additional NMR data on the C-terminus of eEF1Bγ (Vanwetswinkel *et al.*, 2003) leads to a nearly complete although fragmented eEF1 complex. The unique factor eEF3 extends the work on translation elongation to allow a coordinated analysis of the inter-related functions of the translation-elongation machinery. We show that both full-length and truncated factor can be rapidly purified from *Saccharomyces cerevisiae* or *Escherichia coli* and crystallized to give crystals suitable for structure determination. Furthermore, the full-length histidine affinity-tagged form of eEF3 is functional in yeast.

2. Materials and methods

2.1. Cloning and expression of six-histidine-tagged eEF3 and eEF3-980

pTKB602, expressing N-terminally 6×His-tagged eEF3 from a *CEN TRP1* plasmid under its own promoter, was isolated from TKY702

© 2004 International Union of Crystallography
Printed in Denmark – all rights reserved

(Anand *et al.*, 2003). The 5′ primer CGA ATC CAT CGA TAA CAT TAA CAT ATG CAT CAC CAT CAC CAT CAC TCT GAT TCC places an *Nde*I site upstream of the start codon followed by six histidine codons. The 3′ primer adds a *Bam*HI site after the stop codon (5′ CGG GAT CCA AAG ATT AGA ATT CTTCG 3′). To clone 6×His-980-eEF3 in the pET11a vector, the same forward primer was used with a 3′ primer that adds a stop codon at the place of codon 981 followed by a *Bam*HI site. The fragment was PCR amplified using pTKB602 as the template. The resulting plasmids expressing 6×His-eEF3 (pTKB632) and 6×His-980-eEF3 (pTKB630) were transformed into competent *E. coli* BL-21 cells. Cells were inoculated in LB plus ampicillin overnight at 310 K. At an $A_{600\,\mathrm{nm}}$ of 0.6, the culture was induced with IPTG at a final concentration of 1 m*M* for 5 h at 310 K.

In order to facilitate purification from yeast, a 6×His tag was added to the N-terminus of *S. cerevisiae* eEF3 under the control of its own promoter. An *Nde*I site was introduced upstream of the start codon and six histidine codons were introduced after the start codon of eEF3 encoded on plasmid pTKB594 (*TRP1 CEN*) by Quikchange (Stratagene) using the primer 5′ CGA ATC CAT CGA TAA CAT TAA CAT ATG CAT CAC CAT CAC CAT CAC TCT GAT TCC. The resulting yeast expression plasmid pTKB602 was transformed into *S. cerevisiae* strain TKY554 (Anand *et al.*, 2003; Mat*α leu2-3,112 ura3-52 trp1-7 lys2 his4-713 met2-1 yef3::LEU2 pYEF3 URA3 CEN*) and loss of the wild-type eEF3-encoding gene on the *URA3* plasmid was monitored by growth on 5-fluoroorotic acid (Boeke *et al.*, 1987). The resulting strain TKY676 expressing only 6×His-eEF3 was monitored for altered growth at 286, 293 and 310 K as described by Carr-Schmid *et al.* (1999). The expression of 6×His-eEF3 was monitored by Coomassie-staining and Western-blot analysis. 6×His-eEF3 was also cloned into a 2μ *TRP1* plasmid, producing plasmid pTKB628. The overexpression plasmid encoding 6×His-eEF3 was also functional as the only form of the protein. To construct a yeast plasmid expressing 6×His-eEF3-980, the primer 5′ GGT CAC AAC TGG GTT AGT TAA TAA GGT CAA GGT GCT GGT CCA AGA ATC GAT AAG was used with pTKB628 as a template for site-directed mutagenesis by the Quikchange method (Stratagene). The resulting plasmid pTKB724 was transformed in TKY554 and allowed loss of the wild-type eEF3 plasmid (data not shown).

2.2. Purification of eEF3 from *E. coli* or *S. cerevisiae*

To purify the proteins from *S. cerevisiae*, 6×His-eEF3 from TKY702 or 6×His-eEF3-980 (in TKY554) cells were grown in YEPD to an $A_{600\,\mathrm{nm}}$ of 2 and were harvested by centrifugation. For lysis, 20 g of cells was resuspended in 40 ml lysis buffer [20 m*M* Tris–HCl pH 7.6, 500 m*M* KCl, 5 m*M* $MgCl_2$, 0.5 m*M* β-mercaptoethanol, 1 m*M* PMSF, one tablet Complete protease inhibitor (Roche), 10% glycerol] and immediately lysed in a high-pressure homogenizer. The lysate was centrifuged at 12 000 rev min^{-1} in a Sorvall SS34 rotor for 20 min to remove cell debris and then centrifuged at 50 000 rev min^{-1} in a Beckman 60Ti rotor for 1 h 15 min. The supernatant was filtered through a 0.9 μm Versapor filter (Gelman) and loaded onto a 5 ml HiTrap Chelating HP column (Amersham) equilibrated in lysis buffer. After loading, the column was washed with two volumes of Ni buffer (20 m*M* Tris–HCl pH 7.6, 100 m*M* KCl, 5 m*M* $MgCl_2$, 0.5 m*M* β-mercaptoethanol, 0.5 m*M* PMSF, 10% glycerol) containing 20 m*M* imidazole and then eluted with a 50 ml linear gradient of 20–200 m*M* imidazole in Ni buffer. Pooled fractions were diluted in one volume of buffer *Q* (20 m*M* Tris–HCl pH 7.6, 5 m*M* $MgCl_2$, 0.5 m*M* DTT, 0.5 m*M* EDTA, 10% glycerol) and applied onto a 9 ml Source-Q (Amersham) column equilibrated in buffer *Q* containing 50 m*M* KCl. Essentially pure eEF3 was eluted using a linear gradient from 50 to 250 m*M* KCl in buffer *Q*.

2.3. Crystallization and data collection

The purified eEF3 was exchanged into crystallization buffer (20 m*M* Tris–HCl pH 7.6, 75 m*M* KCl, 5 m*M* $MgCl_2$, 0.5 m*M* EDTA, 0.5 m*M* DTT, 1 m*M* ADP) and concentrated to 5.0 mg ml^{-1} in Centricon cells. Crystallization experiments were set up at 277 K using the sitting-drop vapour-diffusion method by mixing 2 μl protein solution with 2 μl reservoir solution. Small brick-shaped crystals appeared with reservoirs containing 43% ammonium sulfate (AmS), 100 m*M* acetic acid (HAc) pH 5.2, 5 m*M* $MgCl_2$. Improved spontaneous nucleation was obtained by mixing 2 μl protein solution with 2 μl 70% AmS, 100 m*M* HAc pH 5.2, 5 m*M* $MgCl_2$ instead of reservoir solution. Crystals reached their final size (200–300 μm) after 4–5 weeks. Crystals were crushed and dialysed against 500 ml 2% HAc for analysis of their content

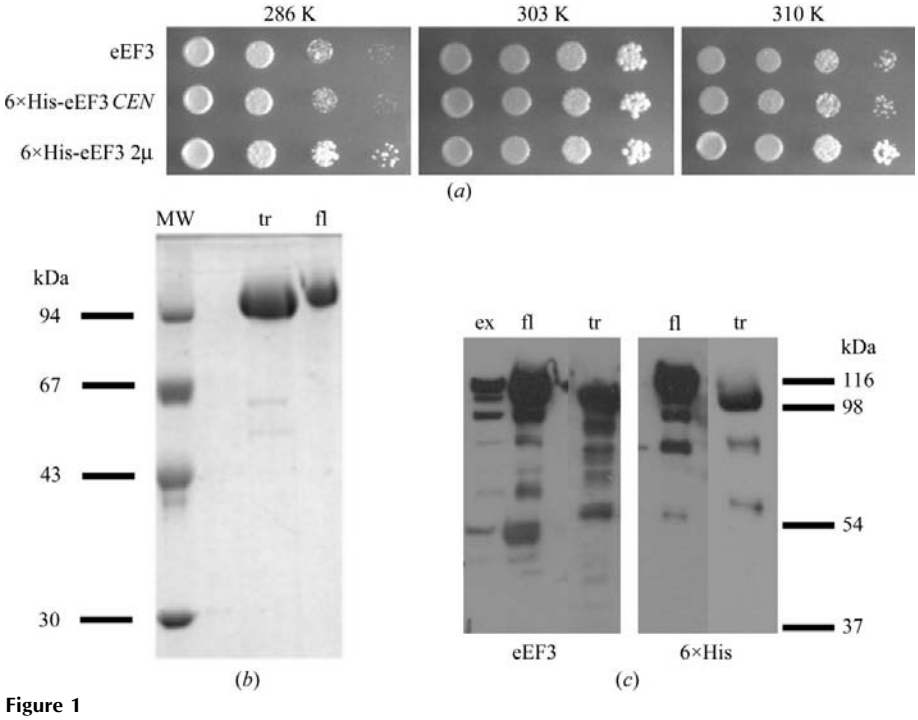

Figure 1
(*a*) Yeast strains TKY554 (wild-type eEF3), TKY676 (6×His-eEF3 *CEN*) and TKY702 (6xHis-eEF3 2μ) were grown overnight in YEPD to an $A_{600\,\mathrm{nm}}$ of 1.0, spotted as tenfold dilutions on YEPD medium and incubated for 2 d at either 286, 303 or 310 K. (*b*) SDS–PAGE of resolubilized crystals of spontanously degraded 6×His-eEF3 (tr) and purified 6×His-eEF3 (fl). (*c*) Western-blot analysis of 6×His-eEF3 and 6×His-eEF3-980. The blot to the left is with an anti-eEF3 antibody against total yeast extract for wild-type eEF3 from TKY554 (ex), 6×His-eEF3 (fl) after Ni-chelate column and 6×His-eEF3-980 (tr) after Ni-chelate column. On the blot to the right an anti-6×His antibody was used.

by MALDI–TOF mass spectroscopy. For preparation of the gold derivative, crystals were harvested in stabilization buffer (50% AmS, 100 m*M* HAc pH 5.2, 5 m*M* $MgCl_2$) and 0.5 m*M* $KAu(CN)_2$ was added to the stabilization buffer and left for 7 d. Prior to data collection, crystals were transferred to cryobuffer (50% AmS, 100 m*M* HAc pH 5.2, 5 m*M* $MgCl_2$, 25% glycerol) and immediately flash-frozen in a nitrogen stream at 100 K or plunged into liquid nitrogen. Data were collected at BW7B (DESY, Hamburg) or ID29 (ESRF, Grenoble). Data were reduced with *MOSFLM*/*SCALA* (Leslie, 1992) or *XDS*/*XSCALE* (Kabsch, 2001). The detection of heavy-atom sites and SIRAS phasing was performed in *CNS* (Brünger *et al.*, 1998) and density modification was performed with the *CCP*4 program *DM* (Cowtan, 1994). The resulting electron density was examined with the graphics program *O* (Jones *et al.*, 1991).

3. Results and discussion

The described purification procedure for eEF3 typically results in 20 mg of crystallizable protein from 6 l of *E. coli* culture and 40 mg from 10 l of *S. cerevisiae* culture (Fig. 1). The addition of a 6×His tag to the N-terminus of eEF3 resulted in a protein able to function as the only form of the protein *in vivo* in a strain where the genomic copy of the *YEF3* gene encoding eEF3 was deleted (Fig. 1*a*). This tagged version produced viable cells whether it was expressed from a low-copy (*CEN*) or high-copy (2µ) plasmid. Analysis of growth of the 6×His-eEF3-expressing strains at a variety of temperatures indicated that these cells grow essentially as wild-type cells at 303 K. Cells expressing 6×His-eEF3 from a *CEN* plasmid show a slight reduction in growth at 310 K (Fig. 1*a* and data not shown). Cells expressing 6×His-eEF3 on high copy had a slight growth advantage at low and high temperatures. Expression of 6×His-980-eEF3, lacking amino acids 981–1044, was efficient in yeast and furthermore resulted in the production of fewer eEF3 proteolytic fragments, as confirmed by Western-blot analysis with antibodies to eEF3 or the 6×His epitope (Fig. 1*c*).

The full-length and truncated tagged forms of the eEF3 coding sequence in the pET11a-based plasmids showed expression in *E. coli*, but the best diffraction was obtained from crystals of eEF3 expressed in yeast. The resulting yeast strain thus provides an efficient system to affinity-purify functional eEF3 and especially of mutant forms of eEF3 for functional and structural studies.

During purification of full-length 6×His-eEF3, we observed a slightly truncated form of eEF3 which crystallized more rapidly and more reproducibly than full-length protein. SDS–PAGE of redissolved crystals showed no further degradation (Fig. 1*b*). This truncated protein did bind to Ni^{2+}-chelating resins, indicating degradation at the C-terminus, which contains several lysine clusters. MALDI–TOF analysis showed a clear peak at 109.4 kDa corresponding to the His tag and the 980 N-terminal residues of eEF3. This prompted us to express the 6×His-eEF3-980. Single crystals of either full-length or truncated eEF3 produced in either *E. coli* or yeast could be grown under very similar conditions and diffracted synchrotron radiation to 3–3.5 Å resolution (Table 1). In order to obtain better experimental phases, we prepared selenomethionine-substituted eEF3 in both *E. coli* and yeast. Crystals of bacterially expressed selenomethionine eEF3 only formed non-diffracting crystals with an altered morphology after several months of incubation. Yeast-expressed selenomethionine 6×His-eEF3-980 formed crystals of normal morphology that diffracted to 2.3 Å resolution (Fig. 2), a significant improvement relative to the normal 3 Å resolution limit from normal eEF3 expressed in yeast. The improvement in resolution may also be caused by the high flux at ESRF ID29; however, this also caused significant radiation damage after 40–50° of data collection. A complete SAD 2.4 Å data set was obtained by merging data from three different crystals (Table 1).

The various data collected show that the unit cell can vary significantly. The long axis in particular is prone to variations and values in the range 199–210 Å have been observed so far. Although a fluorescence scan performed at ESRF ID29 shows a clear

Table 1
Data-collection statistics.

Values in parentheses are for the outer resolution shell. The statistics are calculated with no merging of anomalous pairs for the SeMet and Au data sets and with merged pairs for the native set.

Data set	Selenomethionine	$KAu(CN)_2$	Native
Beamline	ID29, ESRF	BW7B, DESY	BW7B, DESY
Wavelength (Å)	0.9792	0.8431	0.8431
Space group	$P2_12_12_1$	$P2_12_12_1$	$P2_12_12_1$
Unit-cell parameters (Å)	a = 98.783, b = 107.720, c = 209.680	a = 95.587, b = 114.773, c = 202.515	a = 95.710, b = 115.350, c = 202.607
Unique reflections	175271	54138	28522
Resolution (Å)	20–2.4 (2.5–2.4)	20–3.5 (3.6–3.5)	20–3.5 (3.6–3.5)
Completeness (%)	99.0 (94.5)	99.8 (98.7)	98.4 (89.9)
Redundancy	3.93 (3.10)	2.61 (2.57)	4.40 (3.72)
Mean $I/\sigma(I)$	10.27 (4.36)	8.40 (2.91)	14.10 (4.39)
Reflections with $I/\sigma(I) > 3$ (%)	85.8 (60.0)	75.0 (43.6)	81.5 (51.1)
$R_{\rm merge}$† (%)	9.6 (33.2)	8.9 (33.7)	9.9 (30.5)

† $R_{\rm merge} = \sum_h \sum_i |I(h)_i - \langle I(h)\rangle| / \sum_h \sum_i I(h)_i$ for the intensity of reflection h measured i times.

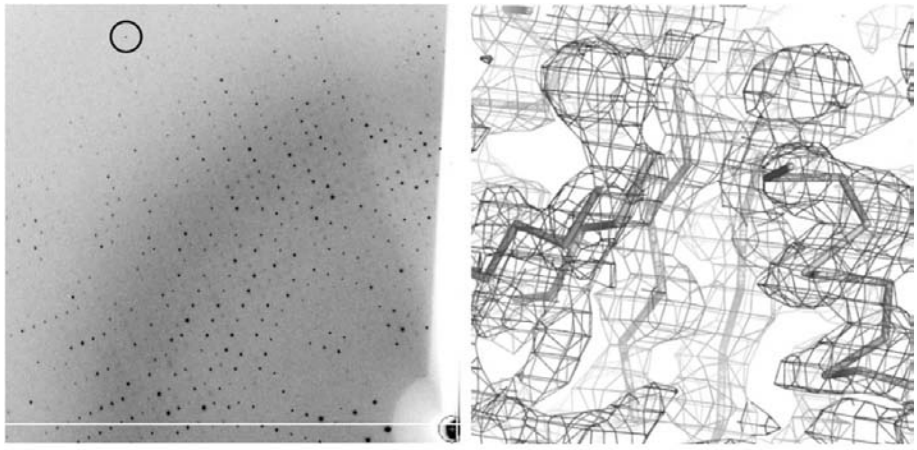

Figure 2
(*a*) Diffraction pattern obtained from the selenomethionine 6×His-eEF3-980 at ID29, ESRF; the circle shows a strong reflection at 2.3 Å resolution. (*b*) The experimental electron density obtained from SIRAS phases followed by density modification including averaging. The map is contoured at 1σ and the secondary elements shown belong to one of the ABC cassettes of eEF3.

anomalous signal and the reduced data shows a moderate signal, we have so far not been able to utilize the anomalous signal for phasing. This is most likely to be a consequence of the low substitution of 65% determined from total amino-acid analysis combined with radiation-induced decay in the diffraction pattern. Similar problems have previously been reported for yeast-expressed selenomethionine protein (Bushnell *et al.*, 2001). With two molecules of eEF3-980 in the asymmetric unit, 44 methionines are present, but only about 15 of these can be located by Patterson search methods.

In contrast, data from the gold derivative has been successfully used for SIRAS phasing. Initially searches identified two major sites, but in *CNS* gradient maps each site decomposes into four separate very close sites. This showed that the asymmetric unit contains two molecules of eEF3 and has a solvent content of 52%. In agreement with prediction, an initial solvent-flattened map showed a large helical domain with HEAT repeats and the presence of two ABC domains. The density was considerably improved by averaging over the two copies of eEF3 (Fig. 2) and the averaged map is currently being used for model building.

We are grateful for assistance during data collection at EMBL, DESY and ID29, ESRF. We also thank Peter Højrup for performing mass spectroscopy and Lars Sottrup-Jensen for total amino-acid analysis. GRA and TGK were supported by Human Frontier Science Program RPG0067/2002 and NIH GM 62789. GRA was supported by the Danish Science Research Council and EU FP5.

References

Anand, M., Chakraburtty, K., Marton, M. J., Hinnebusch, A. G. & Kinzy, T. G. (2003). *J. Biol. Chem.* **278**, 6985–6991.

Andersen, G., Pedersen, L., Valente, L., Kinzy, T., Kjeldgaard, M. & Nyborg, J. (2000). *Mol. Cell*, **6**, 1261–1266.

Boeke, J. D., Trueheart, J., Natsoulis, G. & Fink, G. R. (1987). *Methods Enzymol.* **154**, 164–175.

Brünger, A. T., Adams, P. D., Clore, G. M., DeLano, W. L., Gros, P., Grosse-Kunstleve, R. W., Jiang, J.-S., Kuszewski, J., Nilges, M., Pannu, N. S., Read, R. J., Rice, L. M., Simonson, T. & Warren, G. L. (1998). *Acta Cryst.* D**54**, 905–921.

Bushnell, D. A., Cramer, P. & Kornberg, R. D. (2001). *Structure*, **9**, R11–R14.

Carr-Schmid, A., Durko, N., Cavallius, J., Merrick, W. C. & Kinzy, T. G. (1999). *J. Biol. Chem.* **274**, 30297–30302.

Cowtan, K. (1994). *Jnt CCP4/ESF–EACBM Newsl. Protein Crystallogr.* **31**, 34–38.

Jeppesen, M. G., Ortiz, P., Shepard, W., Kinzy, T. G., Nyborg, J. & Andersen, G. R. (2003). *J. Biol. Chem.* **278**, 47190–47198.

Jones, T. A., Cowan, S., Zou, J.-Y. & Kjeldgaard, M. (1991). *Acta Cryst.* A**47**, 110–119.

Jørgensen, R., Ortiz, P. A., Carr-Schmid, A., Nissen, P., Kinzy, T. G. & Andersen, G. R. (2003). *Nature Struct. Biol.* **10**, 379–385.

Kabsch, W. (2001). *International Tables for Crystallography*, Vol. *F*, edited by M. G. Rossmann & E. Arnold, ch. 25.22.29. Dordrecht: Kluwer Academic Publishers.

Leslie, A. G. W. (1992). *Jnt CCP4/ESF–EACBM Newsl. Protein Crystallogr.* **26**, 27–33.

Merrick, W. C. & Hershey, J. W. B. (1996). *Translational Control*, pp. 31–69. Cold Spring Harbor, NY, USA: Cold Spring Harbor Laboratory Press.

Pérez, J. M. J., Siegal, G., Kriek, J., Hård, K., Dijk, J., Canters, G. W. & Möller, W. (1999). *Structure*, **7**, 217–226.

Sturtevant, J. (2002). *Expert Opin. Ther. Targets*, **6**, 545–553.

Triana-Alonso, F. J., Chakraburtty, K. & Nierhaus, K. H. (1995). *J. Biol. Chem.* **270**, 20473–20478.

Vanwetswinkel, S., Kriek, J., Andersen, G. R., Guntert, P., Dijk, J., Canters, G. W. & Siegal, G. (2003). *J. Biol. Chem.* **278**, 43443–43451.